JOURNAL OF SOLID STATE CHEMISTRY 79, 34–45 (1989)

System $Bi_{2-x}Pb_xPt_{2-x}Ru_xO_{7-z}$: A Pyrochlore Series with a Metal–Insulator Transition

G. MAYER-VON KÜRTHY, W. WISCHERT, R. KIEMEL, AND S. KEMMLER-SACK*

Institut für Anorganische Chemie der Universität Auf der Morgenstelle 18, D-7400 Tübingen, Federal Republic of Germany

AND R. GROSS AND R. P. HUEBENER

Physikalisches Institut, Lehrstuhl für Experimentalphysik II, Auf der Morgenstelle 14, D-7400 Tübingen, Federal Republic of Germany

Received August 31, 1988; in revised form October 28, 1988

The pyrochlore compounds $Bi_2Pt_2O_7$ (insulator) and $Pb_2Ru_2O_{6.5}$ (metallic conductor) form a continuous series of solid solutions $Bi_{2-x}Pb_xPt_{2-x}Ru_xO_{7-z}$. Increasing substitution of the platinum by ruthenium results in a gradual insulator–metal transition. Metallic conductivity is found for a substitution level of $x \gtrsim 1.5$. The presence of variable range hopping conductivity in the insulating regime strongly suggests that the metal–insulator transition is of Anderson type. © 1989 Academic Press, Inc.

1. Introduction

The pyrochlore ruthenates $Pb_2Ru_2O_{6.5}$ and $Bi_2Ru_2O_7$ are applied as the conducting component in thick film resistors (*1, 2*). Due to their high electrical conductivity they have been demonstrated to be effective electrocatalysts for both evolution and reduction of oxygen (*3*). The electrical properties of $Pb_2Ru_2O_{6.5}$ and $Bi_2Ru_2O_7$ have previously been reported (*3*) as well as the band structure, computed self-consistently by using the pseudofunction method (*4*). The pyrochlore platinate $Bi_2Pt_2O_7$, prepared for the first time at normal pressures in (*5*), is an insulator.

This communication deals with the formation of a continuous series of solid solutions $Bi_{2-x}Pb_xPt_{2-x}Ru_xO_{7-z}$ between the end members $Bi_2Pt_2O_7$ and $Pb_2Ru_2O_{6.5}$. Increasing substitution of platinum by ruthenium results in a gradual insulator–metal transition. The presence of variable range hopping conductivity in the insulating regime strongly suggests that the metal–insulator transition is of Anderson type. The resistivity vs temperature data show that there is a gradual variation from a negative to a positive temperature coefficient of resistivity (TCR) as a function of x, suggesting the application of these materials in the fabrication of electrical resistor compositions.

2. Experimental

2.1. Sample Preparation

The end members of the series $Bi_{2-x}Pb_xPt_{2-x}Ru_xO_{7-z}$ with $x = 0$ ($Bi_2Pt_2O_7$)

* To whom correspondence should be addressed.

0022-4596/89 $3.00

TABLE I

LATTICE PARAMETER (Å), DENSITY (g cm^{-3}), MEAN OXIDATION STATE ($\overline{Ox}$) FOR THE SYSTEM $Bi_{2-x}Pb_xPt_{2-x}Ru_xO_{7-z}$

		Density			$\overline{Ox}$		
			Calculated			Calculated	
x	Lattice[a] parameter	Observed[b]	Model 1	Model 2	Observed[c]	Model 1	Model 2
0	10.369	10.86	10.96	10.96	+4.00	+4.00	+4.00
0.25	10.360	10.43	10.69	10.70	+4.08	+4.06	+4.13
0.5	10.351	10.39	10.42	10.45	+4.18	+4.13	+4.25
0.75	10.335	—	10.17	10.21	+4.26	+4.19	+4.38
0.85	10.328	10.06	10.07	10.11	+4.31	+4.21	+4.43
1.0	10.321	9.63	9.92	9.97	+4.36	+4.25	+4.50
1.1	10.313	—	9.81	9.87	+4.39	+4.28	+4.55
1.25	10.302	—	9.66	9.72	+4.39	+4.31	+4.63
1.5	10.290	9.24	9.39	9.47	—	+4.38	+4.75
1.65	10.278	—	9.24	9.32	—	+4.41	+4.83
1.75	10.274	9.20	9.13	9.22	—	+4.44	+4.88
1.9	10.262	8.65	8.98	9.07	—	+4.48	+4.95
2.0	10.255	8.57	8.86	8.97	—	+4.50	+5.00

[a] ±0.003.
[b] ±0.05.
[c] ±0.02.

and $x = 2$ ($Pb_2Ru_2O_{6.5}$) were prepared by solid-state synthesis between the intimately mixed (agate mortar) appropriate quantities of Bi_2O_3 (optipur, Merck), PbO (p.a., Merck), and Pt and Ru (99.9%, Heraeus) in corundum boats (Degussit A123) at 580°C (0.5 hr, 72 hr, $x = 0$) or 700°C (0.5 hr, 12 hr) and 750°C (48 hr, $x = 2$), respectively. The materials were reground several times. The pyrochlores are well crystallized. The lattice constants (Table I) are in excellent agreement with the data in (*3, 5*). For the preparation of $Bi_2Pt_2O_7$ the use of an excess of Bi_2O_3 (25% (*5*)) has proved to be unnecessary.

The conditions for the formation of the solid solutions with $x = 0.25$, 0.5, 0.75, 0.85, 1.0, 1.1, 1.25, 1.5, 1.65, 1.75, and 1.9 are significantly improved by substituting $Bi(NO_3)_3 \cdot 5H_2O$ (DAB 6, Merck) and $Pb(NO_3)_2$ (specpure, Johnson Matthey) for the corresponding oxides Bi_2O_3 and PbO. The appropriate intimate mixtures were heated at first for 0.5 hr at 500 and 600°C, followed by several firings between 600 and 650°C (total heating time: 5 to 7 days). The reactions were interrupted repeatedly for weight controls, X-ray investigations (Philips powder diffractometer, Cu $K\alpha$ radiation, Au standard), and regrindings. The heat treatment was stopped for single-phase compounds with well-developed crystallinity. A summary of the lattice parameters is given in Table I. All compounds reached the calculated weight for the pyrochlore composition. Prolonged heating leads to minor weight losses of about 1%. Heating at higher firing temperatures results in a decomposition of the pyrochlore phase and the formation of metallic platinum. The same holds for $x = 0$.

The platinum pyrochlore $Bi_2Pt_2O_7$ is deep brown. With increasing x the color turns to black.

2.2. Density

The densities of the pyrochlores were determined by the classical method using *n*-octane as the buoyancy fluid and compared to the theoretical density calculated from the cell parameters (Table I) for two borderline cases. For Model 1 (general formula $Bi_{2-x}Pb_xPt_{2-x}Ru_xO_{7-x/4}$) oxygen vacancies are introduced with increasing x, leading to the end member $Pb_2Ru_2O_{6.5}$ ($x = 2$). In Model 2 (general formula $Bi_{2-x}Pb_xPt_{2-x}Ru_xO_7$) the oxygen content of the platinum pyrochlore is conserved. The values for both models are summarized together with the experimental data in Table I.

2.3. Mean Oxidation State and Solubility

For all compounds the solubility in different solvents was investigated. Insolubility was observed in cold and boiling HNO_3, HCl, aqua regia, H_2SO_4, and KOH (30%) for all compositions. On the contrary, solubility is obtained by the action of boiling concentrated HBr for $0 \leq x \leq 1.25$. For these compounds the mean oxidation state ($\overline{Ox}$) of the noble metals has been determined according to (*6*). The results are included in Table I and compared with the calculated values for Models 1 and 2 (Section 2.2.)

2.4. Resistivity Measurements

Four-probe dc conductivity measurements were performed on compacted powder samples at room temperature (RT) and 77 K as well as on pressed and sintered pellets between RT and 77 K. The piston-in-cylinder conductivity cell was fabricated either from ceramic with Au contacts or from laminated paper (Pertinax) with Cu contacts, respectively. The sample was kept under dynamic load (typically 150 MPa applied uniaxial stress (*7*)) in order to ensure good contact and to eliminate possible systematic errors produced by a change in sample compression as the temperature was changed. For the sintered samples intimate electrical contact between the copper wires and the pellet was provided by using silver paint. Typical measuring currents were 1 mA (current source 224, Keithley). The voltage drop across the pair of annular contact points, which were spaced about 10 mm apart, was measured automatically (PC 308, Hewlett Packard) in cyclic permutation (scanner 705, Keithley) with a Model 181 nanovoltmeter (Keithley) using a resolution of 10 nV. During a typical run, the sample resistivity (ρ) was measured at about 10 K intervals during controlled warm-up. Applying first a positive current and then a negative current of the same magnitude allows us to cancel extraneous dc offset voltages by calculating the voltage difference between the voltage across the device for a positive current and that for a negative current. The effective density of the compacted powder samples was between 85 and 93% of the theoretical density. For the pressed and sintered pellets the effective density was typically about 60%. The resistivity of each sample was calculated as follows without any correction for density: $\rho = R_M \times \pi d/\ln 2$ (*8*), where R_M is the average resistance and d the sample thickness.

3. Results and Discussion

3.1. Solid Solution $Bi_{2-x}Pb_xPt_{2-x}Ru_xO_{7-z}$

The platinum pyrochlore $Bi_2Pt_2O_7$ forms a continuous series of solid solutions with $Pb_2Ru_2O_{6.5}$. All members are cubic. For $0 \leq x \leq 1.9$ the observed reflections fulfill the conditions of the pyrochlore space group $Fd3m$. On the contrary in the case of the ruthenate end member $Pb_2Ru_2O_{6.5}$ additional ($hk0$) reflections with $h + k = 2n$ are observed, forbidden in $Fd3m$ but allowed for the $Pb_2Ru_2O_{6.5}$ structure with space group $F43m$ (*9*). The absence of the extra

TABLE II

LATTICE CONSTANTS a (Å), x_O FOR O IN 48f, R' VALUES (%), AND INTERATOMIC DISTANCES (Å) FOR $Bi_{2-x}Pb_xPt_{2-x}Ru_xO_{7-z}$

	$x = 0$ (5)	$x = 0.5$	$x = 1.0$	$x = 1.65$	$x = 1.9$
a	10.369	10.351	10.321	10.278	10.262
x_O	0.350	0.335	0.328	0.323	0.319
R'	4.2	3.4	3.5	3.6	3.7
A–A	3.67	3.66	3.65	3.63	3.63
A–B	3.67	3.66	3.65	3.63	3.63
B–B	3.67	3.66	3.65	3.63	3.63
A–O	2.40	2.50	2.55	2.57	2.60
A–O′	2.25	2.24	2.23	2.23	2.22
B–O	2.11	2.03	1.99	1.97	1.95

($hk0$) reflections with $h + k = 2n$ for all mixed crystals with $0 \leq x \leq 1.9$ implies the adoption of the pyrochlore structure for the whole series with the exception of the pure lead ruthenate. A similar observation holds for the series $Bi_{2-x}Pb_xRu_2O_{7-z}$ (*10*).

The mean oxidation state for platinum and ruthenium ($\overline{Ox}$) is compared with the calculated values for Models 1 and 2 in Table I. The observed $\overline{Ox}$'s always exceed the values for Model 1 but never reach the values for complete oxygen lattice (Model 2). Consequently the compositions with $0.25 \leq x \leq 1.25$ are deficient in oxygen, but the oxygen content is slightly higher than for the case of an ideal solid solution between $x = 0$ ($Bi_2Pt_2O_7$) and $x = 2$ ($Pb_2Ru_2O_{6.5}$), described by Model 1. With the assumption that all platinum rests in the four-valent state, the mean oxidation state of ruthenium stays nearly unchanged at +4.65. This value is slightly higher than for the pure ruthenium pyrochlore $Pb_2Ru_2O_{6.5}$ with $\overline{Ox} = +4.50$.

The density measurements (Table I) are in agreement with the calculated values. No unequivocal decision between Models 1 and 2 is possible due to the small influence of the oxygen content on the formula weight.

For the series $Bi_{2-x}Pb_xPt_{2-x}Ru_xO_{7-z}$ the lattice parameter (Table I) decreases uniformly with increasing x (fulfillment of Végard's law). Note that this contraction is not due to a decrease in ionic radii (Bi^{3+}, 1.17; Pb^{2+}, 1.29; Pt^{4+}, 0.625; Ru^{4+}, 0.620; Ru^{5+}, 0.565 Å (*11*); from the larger value for Pb^{2+} than for Bi^{3+} an opposite trend would be predicted) but mainly to a decrease in the noble metal-to-oxygen distances. Table II shows the results of intensity calculations on powder data for some members of the series $Bi_{2-x}Pb_xRu_{2-x}Pt_xO_{7-z}$. For the space group $Fd3m$ (general formula $A_2B_2O_6O'$) with A in 16d, B in 16c, O in 48f (O) and 8b (O′), and the isotropic temperature factors B_A, 1.7 ($x = 0.5$), 1.9 ($x = 1.0$), 2.0 ($x = 1.65$), 2.3 ($x = 1.90$); B_B, 0.4 ($x = 0.5$ and 1.0), 0.5 ($x = 1.65$), 0.6 ($x = 1.90$); $B_O = B_{O'} = 0.5$ Å^2 ($x = 0.5, 1.0, 1.65, 1.90$) the reliability factor $R' = \Sigma|I_o - I_c|/\Sigma I_c$ is about 4%.

With increasing x the oxygen parameter x_O of O (48f) decreases from 0.350 ($x = 0$) for $Bi_2Pt_2O_7$ (*5*) to 0.319 ($x = 1.9$), approaching the value of the ideal pyrochlore $A_2B_2O_6O'$ with $x_O = 0.3125$ (*12*) more and more. The observed shrinkage of the B–O distances points to an increasing interaction within the octahedral framework of the pyrochlore lattice. A similar observation holds for the solid solution between the insulator $Bi_2Pt_2O_7$ and the metal-like conductor $Bi_2Ir_2O_7$ (system $Bi_2Pt_{2-x}Ir_xO_7$ (*5*)).

Figure 1 shows scanning electron microscopy (SEM) photomicrographs of compressed samples with $x = 0$ (Fig. 1a), 1.0 (Fig. 1b), 1.65 (Fig. 1c), and 2.0 (Fig. 1d). All samples are highly dispersive; the mean grain size is $\lesssim 1$ μm. The energy dispersive X-ray analysis (EDXA) conducted on different sized areas spread over the surface indicated a nearly uniform ($x = 1.0$) or uniform distribution ($x = 1.65, 2.0$) of the elements. For $x = 0$ some occasional inclusions with higher Bi content are detected in the uniform matrix.

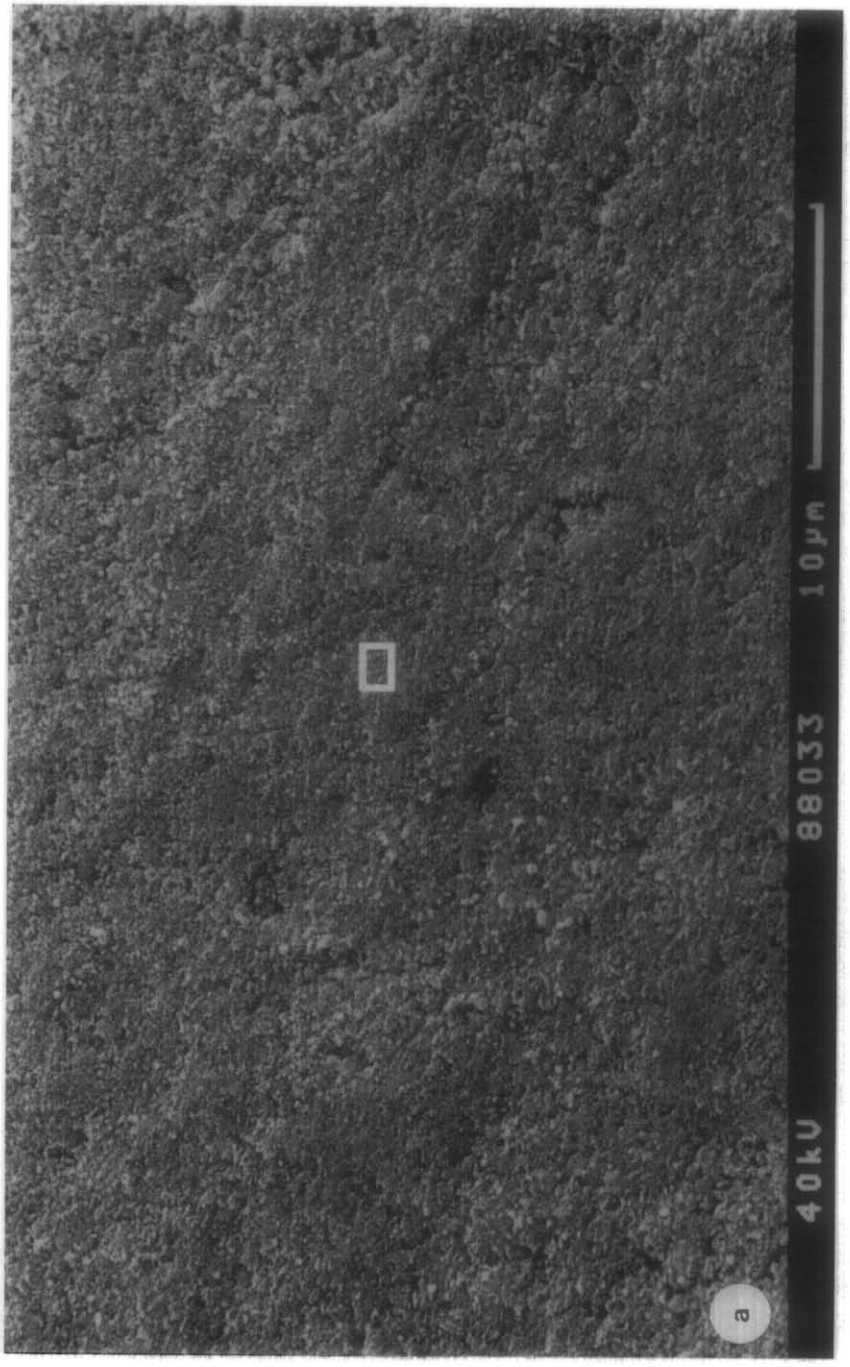

FIG. 1. SEM photomicrographs of compressed samples with $x = 0$ (a), 1.0 (b), 1.65 (c), and 2.0 (d).

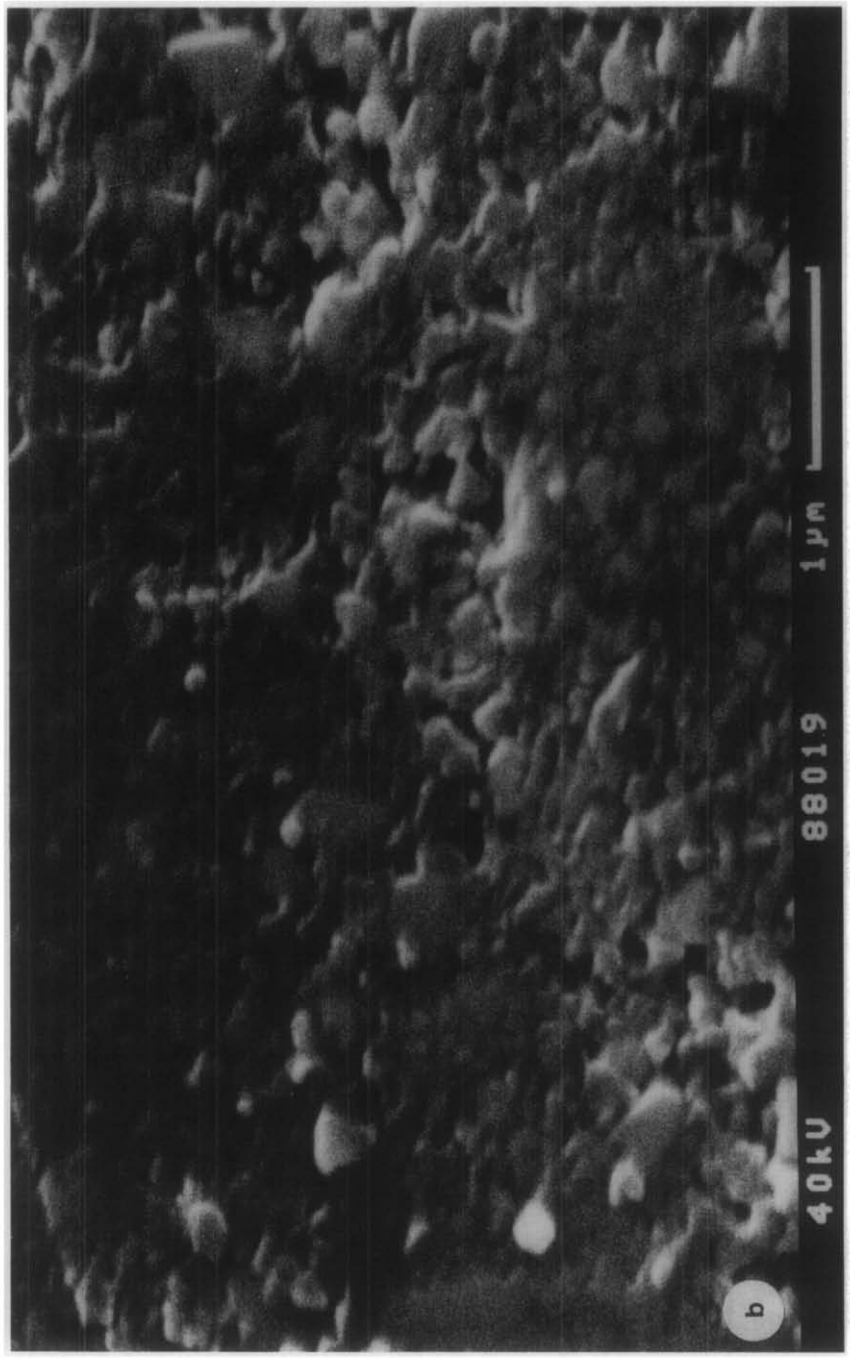

FIG. 1—*Continued*

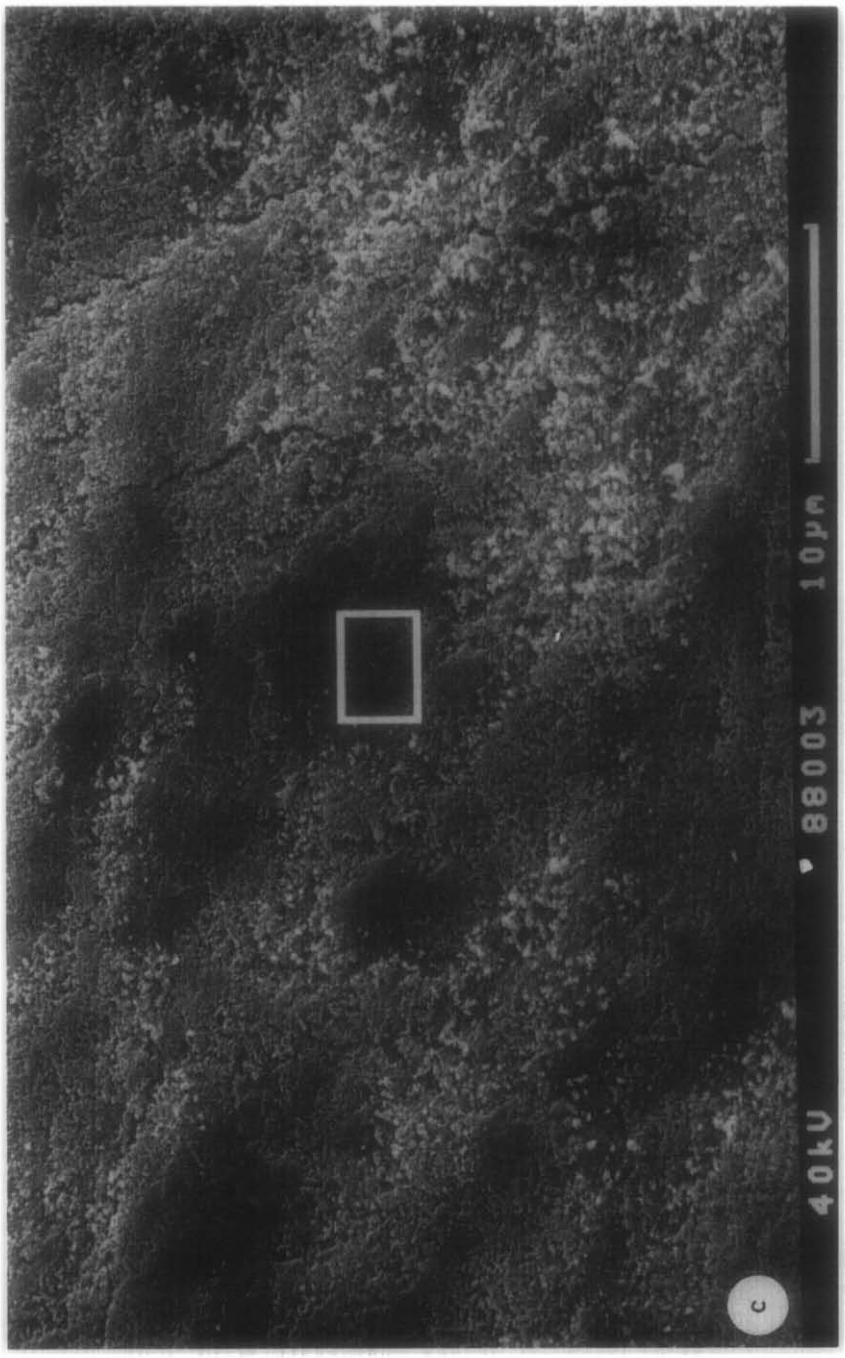

FIG. 1—*Continued*

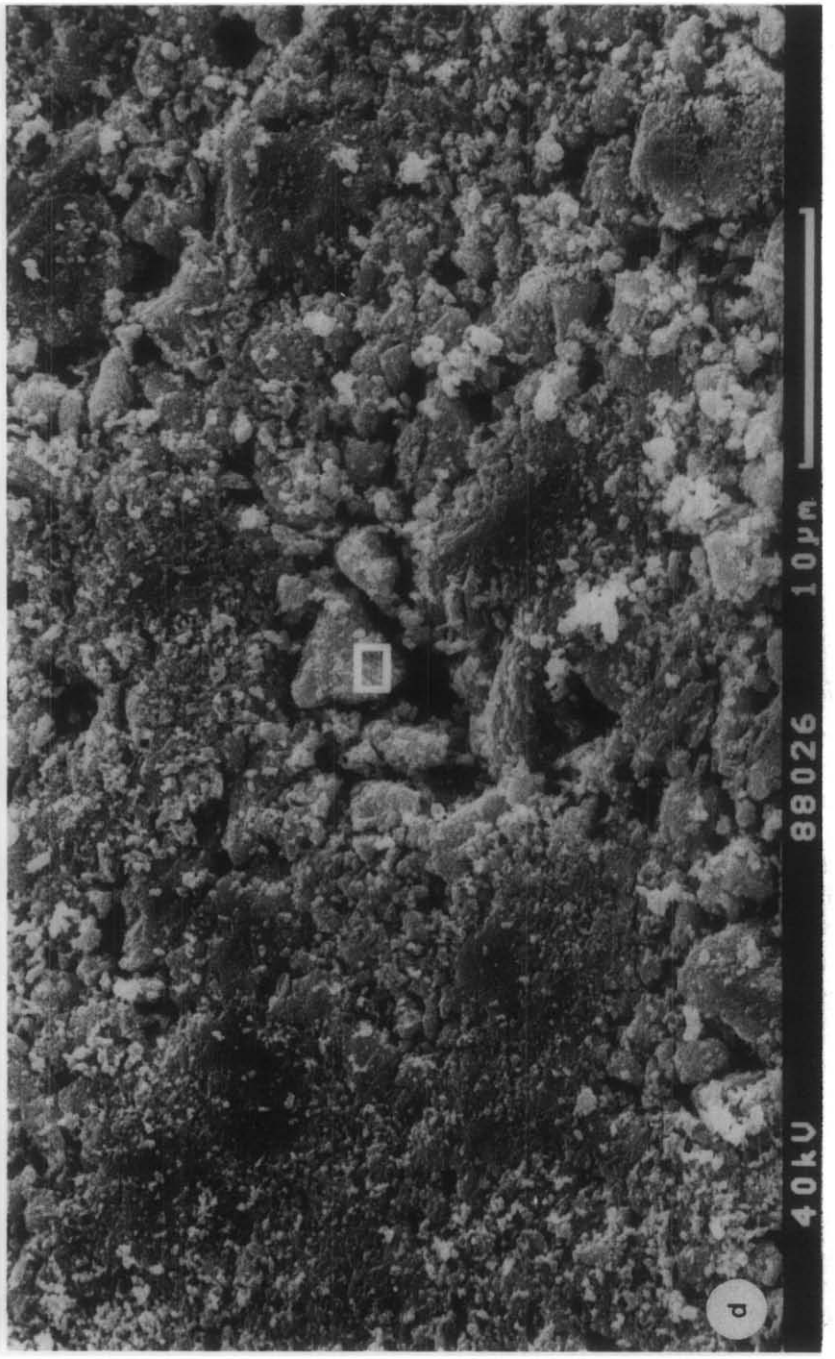

FIG. 1—*Continued*

TABLE III

SELECTED RESISTIVITY AND TEMPERATURE COEFFICIENT OF RESISTIVITY (TCR) VALUES FOR $Bi_{2-x}Pb_xPt_{2-x}Ru_xO_{7-z}$

	Resistivity[a]		
	ρ (ohm cm)		TCR
x	77 K	300 K	(ppm/K)
0	$>10^6$	1.5×10^6	—
0.25	7.2×10^4	1.0×10^6	-3.22×10^6
0.5	1.1×10^1 (4.7×10^1)	6.1×10^{-1} (6.1×10^{-1})	−70,640
0.75	2.7×10^{-1}	3.5×10^{-2}	−30,110
0.85	6.2×10^{-2}	2.3×10^{-2}	− 7,600
1.0	2.5×10^{-2} (3.9×10^{-2})	1.1×10^{-2} (1.1×10^{-2})	− 5,710
1.1	6.1×10^{-3}	4.0×10^{-3}	− 2,350
1.25	7.1×10^{-3}	5.5×10^{-3}	− 1,300
1.5	1.2×10^{-3} (1.5×10^{-3})	1.3×10^{-3} (3.0×10^{-3})	+ 350
1.65	1.0×10^{-3}	1.3×10^{-3}	+ 1,040
1.75	8.7×10^{-4}	1.2×10^{-3}	+ 1,230
1.9	3.1×10^{-4}	5.1×10^{-4}	+ 1,760
2.0	1.8×10^{-4} (1.8×10^{-4})	4.7×10^{-4})	+ 2,770

[a] Values for compacted powder samples given for all compositions; values for pressed and sintered pellets in parentheses.

3.2. *Electrical Properties*

The resistivity measurements (Section 2.4.) were first applied to $Pb_2Ru_2O_{6.5}$ for which conductivity versus temperature data are available in the literature. The results (summarized in Table III and Fig. 2) show excellent agreement between the values obtained from compacted powders and from pressed and sintered pellets (data in parentheses) as well as with the data in the literature (sintered polycrystalline sample: $\rho_{RT} = (2.7 \pm 0.1) \times 10^{-4}$ ohm cm, $\rho_{77\,K} = (0.9 \pm 0.1) \times 10^{-4}$ ohm cm (*13*), $\rho_{RT} = 5 \times 10^{-4}$ ohm cm (*14*), $\rho_{RT} = 3.0 \times 10^{-4}$ ohm cm (*15*); pressed powder sample: $\rho_{RT} = (1.17 \pm 0.02) \times 10^{-3}$ ohm cm (*3*)).

The resistivity data of the pressed powders of the solid solutions are again in excellent agreement with the data for pressed and sintered pellets (Table III). Clearly, one must bear in mind that the electrical properties of polycrystalline bulk samples are highly dependent on sample preparation

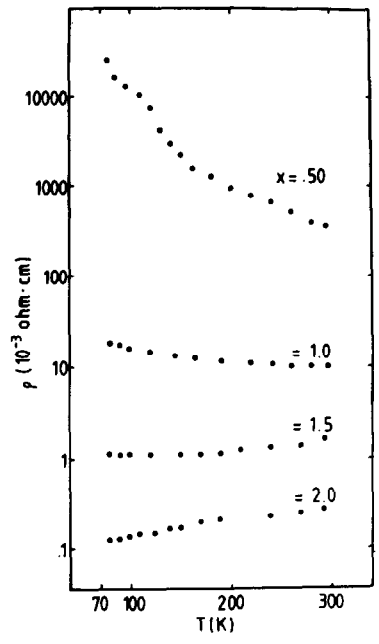

FIG. 2. Resistivity vs temperature for $Bi_{2-x}Pb_xPt_{2-x}Ru_xO_{7-z}$.

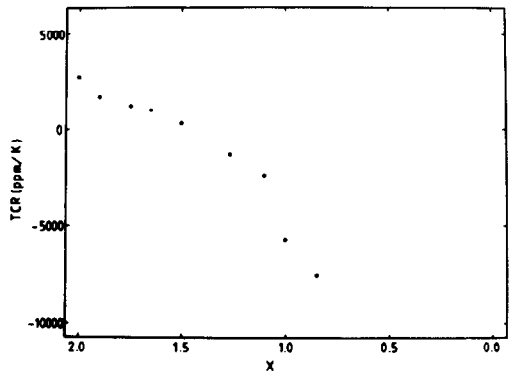

FIG. 3. TCR vs x for $Bi_{2-x}Pb_xPt_{2-x}Ru_xO_{7-z}$.

techniques and only measurements on pure single crystals can be considered accurate indications of the true resistivity. However, the good agreement obtained between the values for compacted powders and pressed and sintered pellets indicates that the measurement techniques just described can be used to establish reliably the conductivity trends in the series $Bi_{2-x}Pb_xPt_{2-x}Ru_xO_{7-z}$.

From the plots of the ρ versus T in Fig. 2 and the resistivity data in Table III it is evident that the compounds with $x > 1.5$ exhibit metallic-like behavior with a positive TCR (TCR = $(1/\rho)$ $(\Delta\rho/\Delta T)$). With decreasing x the positive TCR is reduced (Table III). For $x \leq 1.25$ the TCR is negative and strongly increases with decreasing x. The smooth variation of TCR is shown in Fig. 3 for $2.0 \leq x \leq 0.85$.

The change from metallic to insulating properties with decreasing x is also reflected in the infrared spectra given in Fig. 4. The compounds with $x \geq 1.0$ show a continuous absorption characteristic of a high concentration of free carriers, while the spectra of the compounds with $x \leq 0.85$ show the development of absorption bands with decreasing x. For $Bi_2Pt_2O_7$ ($x = 0$) the well-developed spectrum of a pyrochlore-type compound is obtained (band assignment in (*5*)), due to the insulating properties of this material. Similar observations have been reported for the system $Bi_2Pt_{2-x}Ir_xO_7$ (*5*), $Pb_2[Ru_{2-x}Pb_x]O_{6.5}$ (*3*), for Ru-containing perovskite polytypes as a function of 3d transition metal ion substitution (*16*), and for various perovskites with 3d transition metals (e.g., $LaNi_{1-x}B_xO_3$; B = Cr, Fe, and Co (*17*)). For the systems $LaNi_{1-x}B_xO_3$, Ganguly and Vasanthacharya (*17*) reported that the vibrational features in the infrared spectra disappear when the resistivity is 10^{-1} ohm cm which is two orders of magnitude more than the value of ρ at which the TCR change sign. In the system $Bi_{2-x}Pb_xPt_{2-x}Ru_xO_{7-z}$ a similar trend is observed.

To facilitate the understanding of the resistivity in terms of the electron transport mechanism we have plotted ln σ as a function of $1/T$ in Fig. 5. The conductivity of the

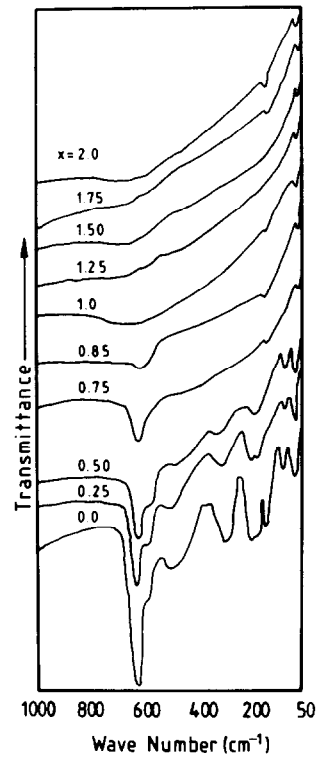

FIG. 4. Infrared spectra for $Bi_{2-x}Pb_xPt_{2-x}Ru_xO_{7-z}$.

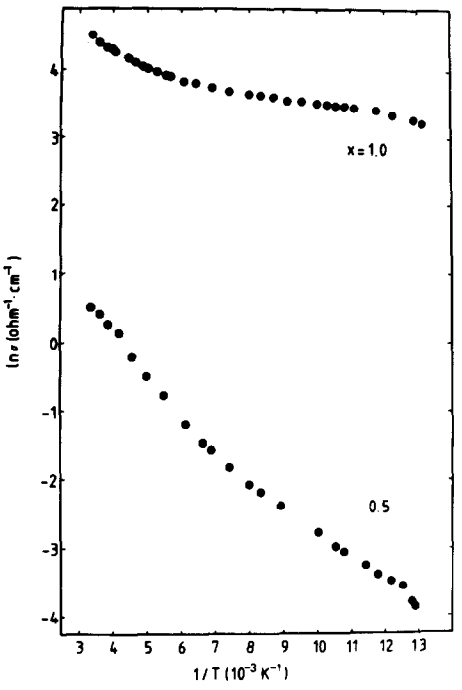

FIG. 5. Electrical conductivity vs reciprocal temperature for $Bi_{2-x}Pb_xPt_{2-x}Ru_xO_{7-z}$.

samples in the insulator side of the metal–insulator transition shows the characteristic thermally activated conduction. However, the activation energy remains temperature dependent. This behavior is highly suggestive of transport by three-dimensional (3D) variable-range hopping (*18*). In Fig. 6 we plotted the conductivity data for $x = 0.5$ and 1.0 as a function of $T^{-1/4}$. Indeed, the conductivity shows a well-defined $T^{-1/4}$ dependence.

4. Conclusions

Electrical conductivity in the pyrochlore $Pb_2Ru_2O_{6.5}$ has been discussed repeatedly (*13, 19–21*). According to recent investigations (*4*) the 6*s* states of Pb are very deep and unlikely to be mixed with the Ru 4*d* states at the Fermi surface. However, the unoccupied Pb 6*p* states are significantly closer to E_F and contribute to the metallic conductivity by mixing with the Ru 4*d* state via the framework oxygen. The same holds for the unoccupied Bi 6*p* states in $Bi_2Ru_2O_7$ (*4*).

For $Bi_2Pt_2O_7$ the t_{2g} states of Pt (Pt^{4+}: t_{2g}^6) are completely occupied and insulating behavior is observed. The doping of $Pb_2Ru_2O_{6.5}$ with Pt^{4+} in the system $Bi_{2-x}Pb_xPt_{2-x}Ru_xO_{7-z}$ is expected to give a break in the conduction pathway within the three-dimensional network of the RuO_6 octahedra leading to a gradual metal–insulator transition (*M–I*). A gradual *M–I* transition has been observed by several workers (*22–24*) in the alkali and alkaline earth doped transition metal oxides. The *M–I* transition is of Anderson type in which the random distribution of the dopants causes sufficient disorder to localize the states in the impurity band and the transition–metal *d* band.

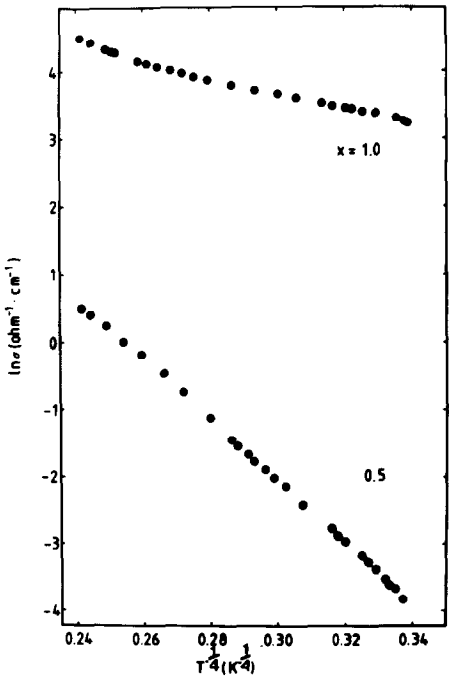

FIG. 6. Electrical conductivity vs $T^{-1/4}$ for $Bi_{2-x}Pb_x$ $Pt_{2-x}Ru_xO_{7-z}$.

A gradual M–I transition has been observed in the systems $Bi_2Pt_{2-x}Ir_xO_7$ (*5*) and $Pb_2[Ru_{2-x}Pb_x]O_{6.5}$ (*3*) as well. It is interesting to note that in these systems as well as in the series $Bi_{2-x}Pb_xPt_{2-x}Ru_xO_{7-z}$ the Ru or Ir content must reach at least an amount of 75% to maintain the metallic conductivity. This substitution level is considerably higher than would be expected from standard percolation models. The criterion of Scher and Zallen for lattices composed of disordered mixtures of metallic spheres of radius R_M and isolating spheres of radius R_i with $R_M = R_i$ gives for the onset of percolation a conducting-volume fraction of 16% (*25*, *26*). The number of unpaired electrons has no influence on the needed value of at least 75% in the pyrochlore systems $Bi_{2-x}Pb_xPt_{2-x}Ru_xO_{7-z}$, $Pb_2Ru_{2-x}Pb_xO_{6.5}$, and $Bi_2Pt_{2-x}Ir_xO_7$. In $Pb_2Ru_2O_{6.5}$, a total amount of five electrons is present in the formula unit in comparison with only two electrons for $Bi_2Ir_2O_7$. The observed smooth variation of the TCR for the series $Bi_{2-x}Pt_{2-x}Ru_xO_{7-z}$ from negative to positive values with increasing x via a nearly temperature-independent TCR for $x \approx 1.5$ suggests the application of these pyrochlores as resistor compositions with tailorable TCR.

Acknowledgments

The authors express their gratitude to the Deutsche Forschungsgemeinschaft for the support of the investigation. We are indebted to the Heraeus GmbH, Hanau for supplying the noble metals. We thank Prof. Dr. E. Lindner and G. Farag for measurement of the far-IR spectra. We thank Mrs. A. Ehmann and Mrs. R. Hüpper for their helpful assistance. We are indebted to the Verband der Chemischen Industrie for valuable support.

References

1. G. E. Pike and C. H. Seager, *J. Appl. Phys.* **48,** 5152 (1977).
2. P. F. Garcia, A. Ferretti, and A. Suna, *J. Appl. Phys.* **5,** 5282 (1982), and references therein.
3. R. A. Beyerlein, H. S. Horowitz, and J. M. Longo, *J. Solid State Chem.* **72,** 2 (1988), and references therein.
4. W. Y. Hsu, R. V. Kasowski, T. Miller, and T.-C. Chiang, *Appl. Phys. Lett.* **52,** 792 (1988).
5. E. Beck and S. Kemmler-Sack, *J. Less-Common Met.* **135,** 257 (1987).
6. B. Krutzsch and S. Kemmler-Sack, *J. Less-Common Met.* **124,** 111 (1986).
7. E. Beck and S. Kemmler-Sack, *Mater. Res. Bull.* **21** 307 (1986).
8. L. J. van der Pauw, *Philips Res. Rept.* **13,** 1 (1958).
9. R. A. Beyerlein, H. S. Horowitz, J. M. Longo, M. E. Leonowicz, J. D. Jorgensen, and F. J. Rotella, *J. Solid State Chem.* **51,** 253 (1984).
10. E. Beck and S. Kemmler-Sack, *J. Less-Common Met.* **113,** 65 (1985).
11. R. D. Shannon, *Acta Crystallogr. Sect. A* **32,** 751 (1976).
12. M. A. Subramanian, G. Aravamudan, and G. V. Subba Rao, *Prog. Solid State Chem.* **15,** 55 (1983).
13. J. M. Longo, P. M. Raccah, and J. B. Goodenough, *Mater. Res. Bull.* **4,** 91 (1969).
14. A. W. Sleight, *Mater. Res. Bull.* **6,** 775 (1971).
15. V. B. Lazarev and I. S. Shaplygin, *Russ. J. Inorg. Chem.* **23**(2), 163 (1978).
16. H.-U. Schaller, A. Ehmann, and S. Kemmler-Sack, *Mater. Res. Bull.* **19,** 517 (1984).
17. P. Ganguly and N. Y. Vasanthacharya, *J. Solid State Chem.* **61,** 164 (1986).
18. N. F. Mott, "The Metallic and Nonmetallic States of Matter" (P. P. Edwards and C. N. R. Rao, Eds.), p. 1, Taylor & Francis, London/Philadelphia (1985).
19. P. A. Cox, R. G. Egdell, J. B. Goodenough, A. Hamnett, and C. C. Naish, *J. Phys. C* **16,** 6221 (1983).
20. R. G. Egdell, J. B. Goodenough, A. Hamnett, and C. C. Naish, *J. Chem. Soc. Faraday Trans.* **79,** 893 (1983).
21. P. A. Cox, J. B. Goodenough, P. J. Tavener, D. Telles, and R. G. Egdell, *J. Solid State Chem.* **62,** 360 (1986).
22. N. F. Mott, *Philos. Mag.* **35,** 11 (1977).
23. P. Dougier and A. Casalot, *J. Solid State Chem.* **2,** 396 (1970).
24. M. Sayer, R. Chen, R. Fletcher, and A. Mansingh, *J. Phys. C* **8,** 2059 (1975).
25. H. Scher and R. Zallen, *J. Chem. Phys.* **53,** 3759 (1970).
26. I. Balberg and N. Binenbaum, *Phys. Rev. B* **35,** 8749 (1987).